

World Journal of *Gastroenterology*

World J Gastroenterol 2021 September 28; 27(36): 5989-6160



FRONTIER

- 5989 Fluorescent cholangiography: An up-to-date overview twelve years after the first clinical application
Pesce A, Piccolo G, Lecchi F, Fabbri N, Diana M, Feo CV

REVIEW

- 6004 Histone methylation in pancreatic cancer and its clinical implications
Liu XY, Guo CH, Xi ZY, Xu XQ, Zhao QY, Li LS, Wang Y
- 6025 Hepatitis B virus infection and hepatocellular carcinoma in sub-Saharan Africa: Implications for elimination of viral hepatitis by 2030?
Amponsah-Dacosta E

MINIREVIEWS

- 6039 Liver disease in the era of COVID-19: Is the worst yet to come?
Mikolasevic I, Bozic D, Pavić T, Ruzic A, Hauser G, Radic M, Radic-Kristo D, Razov-Radas M, Puljiz Z, Milic S
- 6053 Treatment of hepatitis B virus infection in children and adolescents
Stinco M, Rubino C, Trapani S, Indolfi G

ORIGINAL ARTICLE**Basic Study**

- 6064 CircRNA_0084927 promotes colorectal cancer progression by regulating miRNA-20b-3p/glutathione S-transferase mu 5 axis
Liu F, Xiao XL, Liu YJ, Xu RH, Zhou WJ, Xu HC, Zhao AG, Xu YX, Dang YQ, Ji G
- 6079 Exosomal microRNA-588 from M2 polarized macrophages contributes to cisplatin resistance of gastric cancer cells
Cui HY, Rong JS, Chen J, Guo J, Zhu JQ, Ruan M, Zuo RR, Zhang SS, Qi JM, Zhang BH

Case Control Study

- 6093 Evaluation of biomarkers, genetic mutations, and epigenetic modifications in early diagnosis of pancreatic cancer
Rah B, Bandy MA, Bhat GR, Shah OJ, Jeelani H, Kawoosa F, Yousuf T, Afroze D

Retrospective Study

- 6110 Impact of radiogenomics in esophageal cancer on clinical outcomes: A pilot study
Brancato V, Garbino N, Mannelli L, Aiello M, Salvatore M, Franzese M, Cavaliere C

- 6128** Clinicopathological characteristics and longterm survival of patients with synchronous multiple primary gastrointestinal stromal tumors: A propensity score matching analysis

Wu H, Li C, Li H, Shang L, Jing HY, Liu J, Fang Z, Du FY, Liu Y, Fu MD, Jiang KW, Li LP

Observational Study

- 6142** Urotensin II levels in patients with inflammatory bowel disease

Alicic D, Martinovic D, Rusic D, Zivkovic PM, Tadin Hadjina I, Vilovic M, Kumric M, Tokic D, Supe-Domic D, Lupi-Ferandin S, Bozic J

CASE REPORT

- 6154** Inverted Meckel's diverticulum diagnosed using capsule endoscopy: A case report

El Hajra Martínez I, Calvo M, Martínez-Porras JL, Gomez-Pimpollo Garcia L, Rodriguez JL, Leon C, Calleja Panero JL

ABOUT COVER

Editorial Board Member of *World Journal of Gastroenterology*, Mark D Gorrell, BSc, PhD, Professor of Liver Science, Head, Liver Enzymes in Metabolism and Inflammation Program, Centenary Institute, Faculty of Medicine and Health, The University of Sydney, New South Wales 2006, Australia. m.gorrell@centenary.org.au

AIMS AND SCOPE

The primary aim of *World Journal of Gastroenterology* (WJG, *World J Gastroenterol*) is to provide scholars and readers from various fields of gastroenterology and hepatology with a platform to publish high-quality basic and clinical research articles and communicate their research findings online. WJG mainly publishes articles reporting research results and findings obtained in the field of gastroenterology and hepatology and covering a wide range of topics including gastroenterology, hepatology, gastrointestinal endoscopy, gastrointestinal surgery, gastrointestinal oncology, and pediatric gastroenterology.

INDEXING/ABSTRACTING

The WJG is now indexed in Current Contents®/Clinical Medicine, Science Citation Index Expanded (also known as SciSearch®), Journal Citation Reports®, Index Medicus, MEDLINE, PubMed, PubMed Central, and Scopus. The 2021 edition of Journal Citation Report® cites the 2020 impact factor (IF) for WJG as 5.742; Journal Citation Indicator: 0.79; IF without journal self cites: 5.590; 5-year IF: 5.044; Ranking: 28 among 92 journals in gastroenterology and hepatology; and Quartile category: Q2. The WJG's CiteScore for 2020 is 6.9 and Scopus CiteScore rank 2020: Gastroenterology is 19/136.

RESPONSIBLE EDITORS FOR THIS ISSUE

Production Editor: Jia-Hui Li; Production Department Director: Yu-Jie Ma; Editorial Office Director: Ze-Mao Gong.

NAME OF JOURNAL

World Journal of Gastroenterology

ISSN

ISSN 1007-9327 (print) ISSN 2219-2840 (online)

LAUNCH DATE

October 1, 1995

FREQUENCY

Weekly

EDITORS-IN-CHIEF

Andrzej S Tarnawski, Subrata Ghosh

EDITORIAL BOARD MEMBERS

<http://www.wjgnet.com/1007-9327/editorialboard.htm>

PUBLICATION DATE

September 28, 2021

COPYRIGHT

© 2021 Baishideng Publishing Group Inc

INSTRUCTIONS TO AUTHORS

<https://www.wjgnet.com/bpg/gerinfo/204>

GUIDELINES FOR ETHICS DOCUMENTS

<https://www.wjgnet.com/bpg/GerInfo/287>

GUIDELINES FOR NON-NATIVE SPEAKERS OF ENGLISH

<https://www.wjgnet.com/bpg/gerinfo/240>

PUBLICATION ETHICS

<https://www.wjgnet.com/bpg/GerInfo/288>

PUBLICATION MISCONDUCT

<https://www.wjgnet.com/bpg/gerinfo/208>

ARTICLE PROCESSING CHARGE

<https://www.wjgnet.com/bpg/gerinfo/242>

STEPS FOR SUBMITTING MANUSCRIPTS

<https://www.wjgnet.com/bpg/GerInfo/239>

ONLINE SUBMISSION

<https://www.f6publishing.com>

Retrospective Study

Impact of radiogenomics in esophageal cancer on clinical outcomes:
A pilot study

Valentina Brancato, Nunzia Garbino, Lorenzo Mannelli, Marco Aiello, Marco Salvatore, Monica Franzese, Carlo Cavaliere

ORCID number: Valentina Brancato 0000-0002-6232-7645; Nunzia Garbino 0000-0001-6863-7313; Lorenzo Mannelli 0000-0002-9102-4176; Marco Aiello 0000-0002-3676-0664; Marco Salvatore 0000-0001-9734-7702; Monica Franzese 0000-0002-6490-7694; Carlo Cavaliere 0000-0002-3297-2213.

Author contributions: Brancato V performed the research and wrote the manuscript; Franzese M, Mannelli L and Aiello M contributed to the conception and design of the study and to the acquisition and interpretation of the data; Garbino N, Franzese M and Brancato V contributed to the data curation and processing; Franzese M, Salvatore M, Aiello M and Mannelli L revised the article; Cavaliere C designed the research and approved the final version for publication.

Institutional review board

statement: The study was conducted in accordance with the Declaration of Helsinki, and the study protocol was approved by the Ethics Committee of the Istituto Nazionale Tumori "Fondazione G. Pascale (protocol number 1/20).

Informed consent statement:

Patients were not required to give informed consent to the study

Valentina Brancato, Nunzia Garbino, Lorenzo Mannelli, Marco Aiello, Marco Salvatore, Monica Franzese, Carlo Cavaliere, IRCCS SDN, Naples 80143, Italy

Corresponding author: Lorenzo Mannelli, MD, PhD, Professor, IRCCS SDN, Via E. Gianturco, Naples 80143, Italy. mannelilorenzo@yahoo.it

Abstract**BACKGROUND**

Esophageal cancer (ESCA) is the sixth most common malignancy in the world, and its incidence is rapidly increasing. Recently, several microRNAs (miRNAs) and messenger RNA (mRNA) targets were evaluated as potential biomarkers and regulators of epigenetic mechanisms involved in early diagnosis. In addition, computed tomography (CT) radiomic studies on ESCA improved the early stage identification and the prediction of response to treatment. Radiogenomics provides clinically useful prognostic predictions by linking molecular characteristics such as gene mutations and gene expression patterns of malignant tumors with medical images and could provide more opportunities in the management of patients with ESCA.

AIM

To explore the combination of CT radiomic features and molecular targets associated with clinical outcomes for characterization of ESCA patients.

METHODS

Of 15 patients with diagnosed ESCA were included in this study and their CT imaging and transcriptomic data were extracted from The Cancer Imaging Archive and gene expression data from The Cancer Genome Atlas, respectively. Cancer stage, history of significant alcohol consumption and body mass index (BMI) were considered as clinical outcomes. Radiomic analysis was performed on CT images acquired after injection of contrast medium. In total, 1302 radiomics features were extracted from three-dimensional regions of interest by using PyRadiomics. Feature selection was performed using a correlation filter based on Spearman's correlation (ρ) and Wilcoxon-rank sum test respect to clinical outcomes. Radiogenomic analysis involved ρ analysis between radiomic features associated with clinical outcomes and transcriptomic signatures consisting of eight N6-methyladenosine RNA methylation regulators and five up-regulated

because the analysis used anonymous clinical data that were obtained after each patient agreed to treatment by written consent.

Conflict-of-interest statement: The authors declare that there is no conflict of interest in this study.

Data sharing statement: No additional data are available.

Open-Access: This article is an open-access article that was selected by an in-house editor and fully peer-reviewed by external reviewers. It is distributed in accordance with the Creative Commons Attribution NonCommercial (CC BY-NC 4.0) license, which permits others to distribute, remix, adapt, build upon this work non-commercially, and license their derivative works on different terms, provided the original work is properly cited and the use is non-commercial. See: <http://creativecommons.org/licenses/by-nc/4.0/>

Manuscript source: Unsolicited manuscript

Specialty type: Oncology

Country/Territory of origin: Italy

Peer-review report's scientific quality classification

Grade A (Excellent): A
Grade B (Very good): 0
Grade C (Good): C, C
Grade D (Fair): 0
Grade E (Poor): E

Received: March 2, 2021

Peer-review started: March 2, 2021

First decision: June 3, 2021

Revised: June 16, 2021

Accepted: July 30, 2021

Article in press: July 30, 2021

Published online: September 28, 2021

P-Reviewer: Barad AK, Endo S, Hamaya Y

S-Editor: Zhang H

L-Editor: Filipodia

P-Editor: Xing YX



miRNA. The significance level was set at $P < 0.05$.

RESULTS

Of 25, five and 29 radiomic features survived after feature selection, considering stage, alcohol history and BMI as clinical outcomes, respectively. Radiogenomic analysis with stage as clinical outcome revealed that six of the eight mRNA regulators and two of the five up-regulated miRNA were significantly correlated with ten and three of the 25 selected radiomic features, respectively ($-0.61 < \rho < -0.60$ and $0.53 < \rho < 0.69$, $P < 0.05$). Assuming alcohol history as clinical outcome, no correlation was found between the five selected radiomic features and mRNA regulators, while a significant correlation was found between one radiomic feature and three up-regulated miRNAs ($\rho = -0.56$, $\rho = -0.64$ and $\rho = 0.61$, $P < 0.05$). Radiogenomic analysis with BMI as clinical outcome revealed that four mRNA regulators and one up-regulated miRNA were significantly correlated with 10 and two radiomic features, respectively ($-0.67 < \rho < -0.54$ and $0.53 < \rho < 0.71$, $P < 0.05$).

CONCLUSION

Our study revealed interesting relationships between the expression of eight N6-methyladenosine RNA regulators, as well as five up-regulated miRNAs, and CT radiomic features associated with clinical outcomes of ESCA patients.

Key Words: Esophageal cancer; Radiogenomics; Computed tomography; Radiomics; MicroRNAs; N6-methyladenosine

©The Author(s) 2021. Published by Baishideng Publishing Group Inc. All rights reserved.

Core Tip: This is a retrospective study aiming at investigating the relationship between the expression levels of transcriptomic features (eight N6-methyladenosine RNA methylation regulators and five up-regulated microRNAs) and radiomic features extracted from computed tomography images that were significantly associated to clinical outcomes (stage, alcohol history, body mass index) in patients with esophageal cancer. Radiogenomic analysis revealed significant correlations between the expression of the N6-methyladenosine RNA regulators, as well as five up-regulated microRNAs, and several computed tomography radiomic features associated with three investigated clinical outcomes of esophageal cancer patients.

Citation: Brancato V, Garbino N, Mannelli L, Aiello M, Salvatore M, Franzese M, Cavaliere C. Impact of radiogenomics in esophageal cancer on clinical outcomes: A pilot study. *World J Gastroenterol* 2021; 27(36): 6110-6127

URL: <https://www.wjgnet.com/1007-9327/full/v27/i36/6110.htm>

DOI: <https://dx.doi.org/10.3748/wjg.v27.i36.6110>

INTRODUCTION

Esophageal cancer (ESCA) is one of the most common malignancies and ranks sixth as a cause of lethal cancer worldwide[1]. Despite the different types of treatment, ESCA remains a devastating pathology with an overall 5-year survival rate of 15%–25%. The main issue related to ESCA is that, given the late symptoms manifestation, most patients are diagnosed with advanced-stage ESCA characterized by unresectability or metastatic disease, for which the best treatment choices are palliative interventions such as concurrent chemoradiotherapy and combination chemotherapy[2,3]. The majority of ESCAs fall into two main histologic subtypes: Esophageal adenocarcinoma and esophageal squamous cell carcinoma (ESCC)[4]. Imaging plays a key role in each step of the management of ESCA. Computed tomography (CT) plays an important role in the diagnosis, staging and treatment guidance of ESCA. This imaging technique allows to evaluate the loco-regional extension of ESCA by showing the extent of involvement of the esophageal wall by tumor, as well as the tumor invasion of the peri-esophageal fat[5]. Moreover, it is also useful to detect the presence of distant

metastases[6,7]. However, CT has several limitations associated with the ability to evaluate the intra-tumor heterogeneity of the ESCA, as well as in visually distinguishing the post-treatment residual tumor[8,9].

Therefore, since it is well-recognized that information arising from images may be substantially enhanced by quantitative imaging analysis, the radiomics role has rapidly increased in the last decade for cancer applications, including those related to ESCA[10-12]. Radiomics is evolving as medical technology and is currently one of the most interesting research fields. Through radiomics, quantitative data can be extrapolated from diagnostic images, and these extracted parameters (radiomic features) have the potential to identify tumor characteristics[10,11,13]. The innovative field of radiomics could provide opportunities in the management of ESCA patients for improvements in every step of ESCA management[12,14]. Recent studies on CT radiomics in ESCA analyzed CT radiomics features for several steps of ESCA management, such as preoperative stage identification[15] and prediction of response to treatment[3,16].

On the other hand, the emerging clinical relevance of genomics in cancer medicine by applying the next generation sequencing technologies has provided unprecedented opportunities to understand the biological basis of different cancer types, identify genomic biomarkers in carcinogenesis, identify potential bio-molecular targets for drug response and resistance and to guide clinical decision-making regarding the personalized medicine and the clinical practice[17,18].

Gene expression profiling can improve knowledge about the molecular alterations during carcinogenesis. Biomarkers of these molecular alterations, in turn, may be useful in diagnosing cancers, particularly early, curable cancers. Recently, results from gene expression data analyses have made it possible to investigate the complex pathological mechanisms involved in ESCA, with the aim to discover novel molecular markers for tumor diagnosis and to customize therapy based on an individual tumor genetic composition[19-21]. Several microRNA (miRNA), such as miR-93, miR-21, miR-4746 and miR-196a, were evaluated as potential biomarkers for the early diagnosis of cancer, highlighting their diagnostic values[22]. Recently, several studies also suggested that N6-methyladenosine (m6A) methylation can play a crucial role in cancer progression by regulating biological functions that affect noncoding RNA expression[23,24]. In particular, a recent study[25] highlighted the role of m6A methylation regulators aberrantly expressed in ESCA to predict clinical outcomes.

Combining radiomic features with molecular and genomic characteristics can provide insights to characterize tumor phenotype[26]. In this direction, radiogenomics, as a new field that provides clinically useful prognostic predictions by linking molecular characteristics such as gene mutations and gene expression patterns of malignant tumors with medical images, could provide more opportunities in the management of patients with ESCA for improvements in staging, predicting treatment response and survival[7,21]. Based on promising results obtained from preliminary CT-based radiomics studies on ESCA[16,27] and considering the capability of miRNAs as potential biomarkers able to characterize differential expression of different cancer tissues, as well as the critical role of m6A as epigenetic regulator in cancer biology, we aimed to combine these findings in a radiogenomic study, using appropriate variables as clinical endpoints. Specifically, we used the preoperative ESCA stage as a clinical outcome, since the survival of ESCA patients with early stage (stage I-II) could be up to 85%[28]. Additionally, surgical resection, chemoradiation or other optimal therapeutic approaches depend on accurate preoperative staging. Therefore, accurate preoperative staging is important for predicting prognosis and choosing a suitable therapeutic strategy for patients with ESCA[15]. We also used the history of significant alcohol consumption as a clinical outcome, since this is considered as one of the major risk factors for ESCA[29]. Lastly, we evaluated body mass index (BMI) as a clinical outcome, due to its association with increased risk of ESCA[30,31].

Using publicly available integrated ESCA cohort from The Cancer Genome Atlas (TCGA) and The Cancer Imaging Archive (TCIA)[32,33], we aimed at investigating possible relationships between CT-radiomic features associated with the three above-mentioned clinical outcomes and correlated with esophageal up-regulated miRNAs, which were *in silico*-validated from Zeng *et al*[22], in order to evaluate potential biomarkers for the early diagnosis of ESCA. Furthermore, we evaluated if the same CT-radiomics features could be associated with epigenetic signatures, considering m6A RNA methylation regulators-based prognostic signature for ESCA from Xu *et al* [25] in order to support important information for developing diagnostic and therapeutic strategies.

MATERIALS AND METHODS

Patient population and definition of clinical outcomes

The study was conducted in accordance with the Declaration of Helsinki, and the study protocol was approved by the Ethics Committee of the Istituto Nazionale Tumori “Fondazione G. Pascale (protocol number 1/20). Sixteen patients with diagnosed ESCA were extrapolated by combining the public databases TCIA-TCGA and included in this study[32,33]. All subjects performed CT investigation with iodized contrast medium injection. Of 16 patients, one was excluded due to the presence of artifacts on acquired images. Due to their availability for all 15 patients, the transcriptome profiling and the following clinical variables were extracted and considered as outcomes for this study: Cancer stage, history of significant alcohol consumption and BMI value. We did not perform analyses on smoking measurements (tobacco history, age at starting smoking, pack-year smoked) due to the incompleteness of these data. To perform radiogenomic analyses, we divided patients into two groups according to stages I–II or III–IV, making stage outcome binary. Refer to [Table 1](#) for clinical characteristics and outcomes of included patients.

Image acquisition and processing

CT examinations were acquired on GE Medical Systems (9 patients) and Siemens (6 patients) CT scanner, with slice thickness ranging from 1.25 mm to 2.5 mm and pixel size varying from 0.67 to 0.9. three-dimensional (3D) regions of interest (ROIs) encompassing the tumor were manually delineated slice-by-slice by using ITK-SNAP (version 3.6.0, <http://www.itksnap.org>) on the post-administration of contrast agents CT images. The tumor localization was divided into three regions: 7 patients presented lesions at the middle level, 2 subjects in the middle/distal area and 6 patients in the distal esophagus.

Gray-levels normalization was not performed, since CT gray values reflect absolute world values (Hounsfield units) and should be comparable between scanners. To correct variability from parameters related to voxel size and so unify voxel size across the cohort, radiomics data were extracted from images resampled to isotropic voxels of $1 \times 1 \times 1 \text{ mm}^3$ using B Spline interpolator.

Radiomic analysis

Radiomic features extraction: A total of 1302 radiomics features were extracted from segmented ROIs by using the open source Python package PyRadiomics (<https://pyradiomics.readthedocs.io/en/Latest/>). The extracted radiomics features were categorized into five groups: (1) Shape features ($n = 14$); (2) First-order features including 18 intensity statistics; (3) 74 multi-dimensional texture features including 23 gray level co-occurrence matrix (GLCM), 16 gray level size zone matrix (GLSZM), 16 gray level run length matrix (GLRLM), 14 gray level dependence matrix (GLDM) and 5 neighboring gray tone difference matrix (NGTDM) features; 1196 transformed first-order and textural features including; (4) 736 wavelet features in frequency channels LHL, LLH, HHH, HLH, HLL,HHL, LHH and LLL, where L and H are low- and high-pass filters, respectively; and (5) 460 LoG filtered features with sigma ranging from 1.0 and 5.0, with step size = 1. Features of groups (2) and (3) were grouped together and, from now on, this group will be referred to as “original features”. The extracted radiomics features grouped by similarity in four categories are listed in the [Supplementary Table 1](#). The computing algorithms can be found at www.radiomics.io and the image biomarker standardization initiative presented a document to standardize the nomenclature and definition of radiomic features[34].

Radiomic features selection: Features selection was performed separately for shape features, original features, wavelet features and LoG filtered features in two steps, followed by a third step involving the whole set of features passed through the step I and II. In the first step, a correlation filter based on the absolute values of pairwise Spearman’s correlation (ρ) coefficient was used to reduce feature redundancy. Threshold for ρ was set to 0.8. Briefly, if two features had $\rho > 0.8$, the function looks at the mean absolute correlation of each variable and the variable with the largest mean absolute correlation is removed. The second step varied according to the type of outcome variables. For binary outcomes, a further feature restriction through a univariate analysis was performed by using non-parametric Wilcoxon rank-sum test to investigate the statistical significance with respect to the outcome. Statistical significance was set to $P < 0.05$. The significantly different features were then selected and further reduced in the third step. For continuous outcomes, the second step

Table 1 Characteristics of included patients

Clinical characteristic	Value
Age (mean ± SD)	56.8 ± 8.65
Sex, <i>n</i> (%)	
Male	12 (20)
Female	3 (80)
Histologic diagnosis, <i>n</i> (%)	
EAC	2 (13.3)
ESCC	13 (86.7)
Cancer stage, <i>n</i> (%)	
I-II	4 (26.7)
III-IV	11 (73.3)
TNM staging	
Primary tumor (T)	
T1	3 (20)
T2	2 (13.3)
T3	8 (53.4)
T4	2 (13.3)
Regional lymph nodes (N)	
N0	4 (26.7)
N1	6 (40)
N2	3 (20)
N3	2 (13.3)
Distant metastases (M)	
M0	12 (80)
M1	3 (20)
Alcohol history, <i>n</i> (%)	
Yes	8 (53)
No	7 (47)
Smoking history, <i>n</i> (%)	
Lifelong non-smoker	1 (6.6)
Current smoker	7 (46.6)
Current reformed smoker	2 (13.3)
Current reformed smoker for > 15 yr	1 (6.6)
NA	4 (26.6)
Age at starting smoking	
Under 18 yr old	6 (40)
Over 18 yr old	3 (20)
NA	6 (40)
Pack-year smoked	
Under 10	6 (40)
Over 10	3 (20)
NA	6 (40)

BMI (mean \pm SD)	20.8 \pm 3.55
---------------------	-----------------

BMI: Body mass index; EAC: Esophagus adenocarcinoma; ESCC: Esophagus squamous cell carcinoma; TNM: tumor, node, and metastasis classification (classification of malignant tumors).

consisted of computing ρ between each feature selected through the step I and the reference outcome. Then, all features with a significant $\rho > 0.5$ and P value < 0.05 were considered. In order to check for redundancies among features belonging to the different four groups, the third step consisted in applying the correlation filter described in step I to the whole feature set passed through step II. All steps were implemented using Matlab R2020a (The MathWorks Inc., Natick, MA, United States).

Predictive models building and analysis for stage assessment: In order to evaluate the predictive power of CT radiomic features taken by them for ESCA staging, a fourth step of feature selection was performed for features that were associated with stage. The latter step consisted in ranking the remaining features based on the mutual information (MI) between the distribution of the values of a certain feature and the membership to a particular class. Features were evaluated independently, and the final feature selection occurred by aggregating the five top ranked ones[35-37]. For the binary stage I-II/stage III-IV classification task, the reduced feature set was used to build logistic regression models of order from 1 to 5 that would best predict ESCA stage by using an imbalanced-adjusted bootstrap resampling (IABR) approach on 1000 bootstrap samples[38]. Specifically, the training set was made up 1000 bootstrap samples randomly drawn with replacement from the available dataset. The testing set consisted of the instances that did not belong to the bootstrap sample. Then, application of the imbalance-adjustment step made the probability of picking a positive and a negative instance in the bootstrap sample the same[39-41].

For each model order, the combination of features maximizing the 0.632+ area under the receiver operating characteristic curve (AUC) within 1000 bootstrap training and testing samples was identified. Finally, IABR on 1000 samples was performed again for all models to assess prediction performances[38,42].

Additional analyses were performed starting from the first two, three and four features surviving after the MI-based feature selection step (which was used to build logistic regression models of order from 1 to 2, 1 to 3 and 1 to 4, respectively) that would best predict ESCA stage. Moreover, given that the overall stage is determined after the cancer is assigned categories describing the tumor (T), node (N) and metastasis (M) categories, we tested the capability of these features for predicting T and N status. Analyses assuming M status as clinical outcome were not performed due to the extremely unbalanced sample. Patients were divided into two groups according to T1-T2 or T3-T4 tumor status, making T stage outcome binary. Similarly, we evaluated if CT radiomic features could assess N status by dividing patients into two groups according to the absence (N0) or presence (N1-N2-N3) lymph node status[43].

Transcriptomic data collection

RNA-Seq and miRNA-Seq data of esophageal carcinoma of tumor tissues were downloaded from the GDC Data Portal (<https://gdc-portal.nci.nih.gov/>) considering for TCGA-ESCA project only patients with associated imaging data from TCIA database (see [Supplementary Tables 2 and 3](#) for Clinical and Transcriptomic data, respectively). The mRNAs expression levels were considered as read count based on gene length and the total number of mapped reads (FPKM values). Moreover, miRNA expression quantification was downloaded and normalized counts in reads-per-million-miRNA-mapped were considered.

Radiogenomic analysis

An integrative study design was defined (see [Figure 1](#) for the flowchart reporting the organization of data and analyses in the study) and reported as radiogenomic workflow in [Figure 2](#) in order to evaluate potential association between significant radiomic features according to selected clinical variables (stage, history of significant alcohol consumption and BMI) with biomarkers and RNA regulators characterizing esophageal cancer. For this purpose, a Spearman's correlation analysis was investigated between radiomic features selected after the three features selection steps described above and transcriptomic signatures suggested by Zeng *et al*[22] and Xu *et al* [25]. Specifically, we calculated ρ between the whole selected feature set and the eight

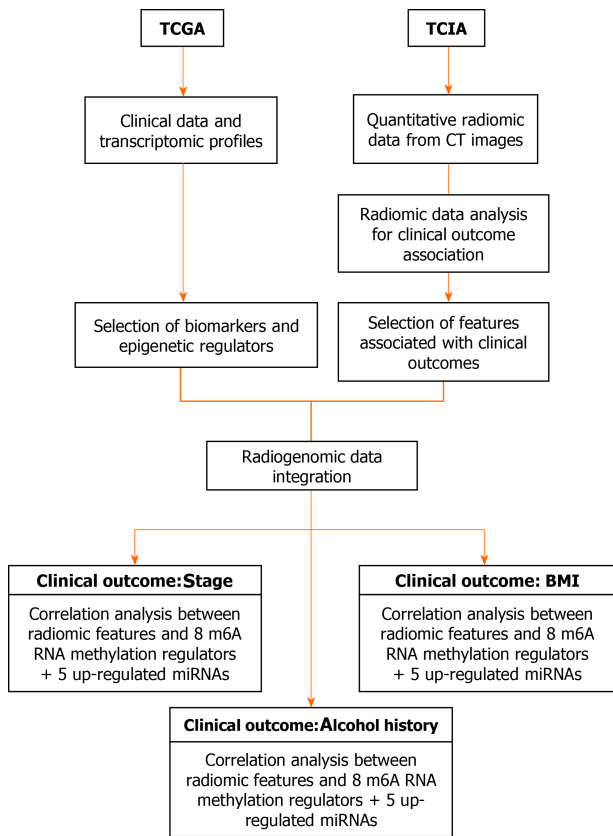


Figure 1 Flowchart reporting the organization of data and analyses in the study. BMI: Body mass index; CT: Computed tomography; TCGA: The Cancer Genome Atlas; TCIA: The Cancer Imaging Archive.

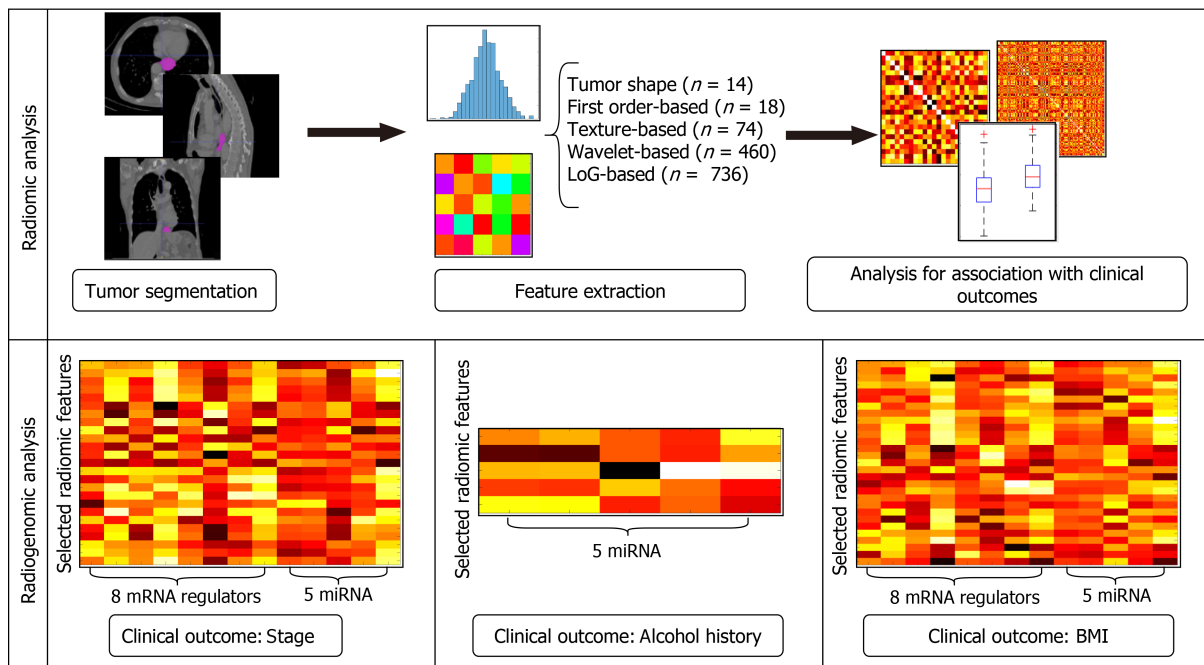


Figure 2 Workflow of radiogenomic analysis implemented in the study. On the first row the radiomic analysis steps. On the second row the radiogenomic analysis for each clinical outcome. BMI: Body mass index; miRNA: MicroRNA; mRNA: Messenger RNA.

m6A RNA methylation regulators (KIAA1429, HNRNPC, RBM15, METTL3, WTAP, YTHDF1, YTHDC1, YTHDF2), as well as ρ between the whole selected feature set and the five up-regulated miRNAs (miRNA-93, miRNA-21, miRNA-4746, miRNA-196a-1, miRNA-196a-2). The significance level was set to 0.05. All analyses were performed

using Matlab R2020a. The statistical methods of this study were reviewed by our bioinformatics and biostatistics group of our research support center.

RESULTS

Radiomic analysis

Radiomic feature selection: None of the 14 shape features passed the step II of features selection, both considering binary outcomes (namely stage and alcohol history) and BMI. So, radiogenomic analysis was not performed for this feature group. Concerning original, wavelet and Log sigma feature groups, the step I of feature selection reduced the feature sets from 92, 736 and 460 to 23, 127 and 65, respectively. Concerning stage analysis, Wilcoxon rank-sum test used in step II of feature selection revealed significant results for 26 radiomic features, of which 25 belonging to the wavelet feature set and the remaining one was the original first order maximum value. However, the latter feature did not pass the second correlation filter of step III (refer to [Table 2](#)). Considering the presence of alcoholic history as clinical outcome, Wilcoxon rank-sum test revealed significant results for five features, of which one belonging to original feature set (Kurtosis) and the remaining ones to wavelet feature set. These five features passed step III, since Kurtosis showed a correlation lower than 0.8 with all four wavelet features (refer to [Table 2](#)). Lastly, considering BMI as the clinical outcome, 26 wavelet and three LoG sigma features were selected due to a significant $p > 0.5$ ($P < 0.05$) with BMI. In total, 29 radiomic features (see [Table 3](#)) survived after the second correlation filter and were associated with the three examined clinical outcomes.

Predictive models building and analysis for stage assessment: The top five features selected after the MI-based feature selection step were wavelet LLH GLDM high gray level emphasis, LLH NGTDM complexity, HHH GLCM joint entropy, HLH entropy and HLL GLCM cluster prominence. Prediction performances of multivariable logistic regression models for the stage I-II/stage III-IV classification task were very high for both five model orders. However, by inspecting prediction performances values in [Table 4](#), we determined that the simplest multivariable model with the best prediction performances were reached by the second order model (AUC = 87%, sensitivity = 64%, specificity = 83% and accuracy = 79%), which was based on wavelet LLH NGTDM complexity and HHH GLCM joint entropy. These results were also confirmed by additional analyses ([Supplementary Tables 4-6](#)). The top five features were also found to be able to predict T and N staging, with best AUCs (0.79 and 0.80, respectively) reached by second order models (see [Supplementary Tables 7 and 8](#) for analyses involving five features). Results of additional analyses for T and N prediction by using two, three and four features are reported in [Supplementary Tables 9-11](#) (T staging) and [Supplementary Tables 12-14](#) (N staging).

Radiogenomic analysis

Stage: Overall, radiogenomic analysis revealed that six of the eight mRNA regulators were significantly correlated with 10 of the 25 selected radiomic features, which were all belonging to the wavelet group. In particular, HRNPC and WTAP were positively correlated with wavelet HHL NGTDM strength ($\rho = 0.61$, $\rho = 0.61$, $P < 0.05$, respectively); METTL3 was positively correlated with wavelet LHL GLDM high gray level emphasis, HLL GLRLM gray level variance, HLL GLDM dependence entropy and LLL GLDM small dependence high gray level emphasis ($\rho = 0.54$, $\rho = 0.53$, $\rho = 0.56$, $\rho = 0.6$, $P < 0.05$, respectively) and negatively correlated with wavelet HLL GLCM inverse variance ($\rho = -0.6$, $P < 0.05$); YTHDF1 reported a positive and significant correlation with the wavelet feature HLL GLCM maximum probability ($\rho = 0.6$, $P < 0.05$) and a negative correlation with HLL 90th percentile ($\rho = -0.61$, $P < 0.05$); YTHDF2 was positively correlated with the wavelet feature HHH GLCM contrast and HHH GLSZM zone percentage ($\rho = 0.57$, $\rho = 0.56$, $P < 0.05$, respectively); the latter feature was also positively correlated with YTHDC1 ($\rho = 0.6$, $P < 0.05$). Moreover, correlation analysis with the five up-regulated miRNA revealed a significant positive correlation between miRNA-93 and two radiomic features, namely wavelet LHL GLDM high gray level emphasis ($\rho = 0.69$, $P < 0.05$) and HHH GLCM joint entropy ($\rho = 0.58$, $P < 0.05$). Notably, HHH GLCM joint entropy contributed to building the best predictive models for stage assessment, as well as T and N assessment. Finally, a positive correlation between miRNA-4746 and HHL GLCM cluster shade was found ($\rho = 0.53$, $P < 0.05$). The radiogenomic results for stage are shown through a heatmap in the [Figure 3](#).

Table 2 Selected radiomic features after the three feature selection steps for binary outcomes

Selected radiomic features, stage	Stage I-II, mean ± SD	Stage III-IV, mean ± SD	P value
Wavelet-HLH first order entropy	0.62 ± 0.13	0.21 ± 0.31	0.031
Wavelet-LHL GLDM high gray level emphasis	0.59 ± 0.32	0.21 ± 0.21	0.044
Wavelet-HLL GLDM high gray level run emphasis	0.67 ± 0.37	0.2 ± 0.18	0.019
Wavelet-HLL GLDM gray level variance	0.74 ± 0.29	0.22 ± 0.29	0.007
Wavelet-HLL GLDM cluster prominence	0.59 ± 0.36	0.14 ± 0.3	0.019
Wavelet-HLL GLDM inverse variance	0.27 ± 0.3	0.68 ± 0.23	0.028
Wavelet-HLL GLDM maximum probability	0.14 ± 0.17	0.58 ± 0.32	0.042
Wavelet-HLL GLDM dependence entropy	0.78 ± 0.18	0.42 ± 0.25	0.028
Wavelet-HLL GLDM dependence variance	0.2 ± 0.21	0.48 ± 0.26	0.044
Wavelet-HLL GLSZM size zone non uniformity	0.69 ± 0.39	0.15 ± 0.15	0.028
Wavelet-HLL GLSZM small area low gray level emphasis	0.02 ± 0.03	0.24 ± 0.33	0.041
Wavelet-HLL first order 90 percentile	0.55 ± 0.39	0.17 ± 0.16	0.029
Wavelet-HHH GLRLM gray level non uniformity normalized	0.39 ± 0.27	0.87 ± 0.19	0.007
Wavelet-HHH GLCM joint entropy	0.68 ± 0.22	0.2 ± 0.27	0.021
Wavelet-HHH GLCM Contrast	0.78 ± 0.19	0.45 ± 0.25	0.021
Wavelet-HHH GLSZM gray level variance	0.91 ± 0.11	0.3 ± 0.39	0.021
Wavelet-HHH GLSZM zone percentage	0.83 ± 0.13	0.35 ± 0.34	0.029
Wavelet-HHH first order 10 percentile	0.11 ± 0.08	0.46 ± 0.35	0.029
Wavelet-HHL NGTDM strength	0.66 ± 0.3	0.28 ± 0.3	0.044
Wavelet-HHL GLCM cluster shade	0.51 ± 0.49	0.04 ± 0.03	0.007
Wavelet-HHL first order Entropy	0.68 ± 0.33	0.27 ± 0.21	0.029
Wavelet-HHL first order mean absolute deviation	0.66 ± 0.35	0.25 ± 0.18	0.029
Wavelet-LLH NGTDM complexity	0.23 ± 0.13	0.13 ± 0.29	0.044
Wavelet-LLH GLDM high gray level emphasis	0.34 ± 0.23	0.14 ± 0.29	0.044
Wavelet-LLL GLDM small dependence high gray level emphasis	0.67 ± 0.32	0.25 ± 0.22	0.029
Selected radiomic features (alcohol history)	No alcohol history (mean ± SD)	Alcohol history (mean ± SD)	P value
Original first order kurtosis	0.37 ± 0.32	0.12 ± 0.12	0.037
Wavelet-LHH first order interquartile range	0.24 ± 0.24	0.5 ± 0.25	0.049
Wavelet-LHH first order mean	0.94 ± 0.04	0.75 ± 0.31	0.013
Wavelet-HHL first order median	0.62 ± 0.2	0.37 ± 0.19	0.026
Wavelet-LLH first order uniformity	0.68 ± 0.27	0.41 ± 0.26	0.037

The first column includes the two binary clinical outcomes investigated in this study (stage, alcohol history). GLCM: Gray level co-occurrence matrix; GLDM: Gray level dependence matrix; GLRLM: Gray level run length matrix; GLSZM: Gray level size zone matrix; H: High-pass filter; L: Low-pass filter; NGTDM: Neighboring gray tone difference matrix; SD: Standard deviation.

Alcohol history: From the integrated analysis, none of the five selected radiomic features was significantly correlated with any of eight RNA regulators (data not shown). Conversely, correlation analysis with the five up-regulated miRNA revealed a significant correlation between the wavelet feature LHH first order Mean and three up-regulated miRNA, namely miRNA-21 ($\rho = -0.56, P < 0.05$), miRNA-4746 ($\rho = 0.64, P < 0.05$) and miRNA-93 ($\rho = 0.61, P < 0.05$), as reported in the heatmap in **Figure 4**.

Table 3 Selected radiomic features after the three feature selection steps for body mass index

Selected radiomic features	mean ± SD	ρ	P value
Wavelet-HLH GLCM IMC2	0.46 ± 0.31	0.6	0.017
Wavelet-HLH GLCM MCC	0.33 ± 0.27	0.67	0.006
Wavelet-HLH first order median	0.59 ± 0.28	-0.56	0.029
Wavelet-HLH first order entropy	0.32 ± 0.33	0.63	0.013
Wavelet-HLH first order root mean squared	0.44 ± 0.31	0.71	0.003
Wavelet-HLH first order skewness	0.5 ± 0.33	0.52	0.049
Wavelet-HLH first order mean absolute deviation	0.54 ± 0.29	0.62	0.013
Wavelet-LHL GLCM IDN	0.77 ± 0.29	0.58	0.023
Wavelet-LHL GLDM high gray level emphasis	0.31 ± 0.29	0.54	0.039
Wavelet-HLL GLRLM high gray level run emphasis	0.32 ± 0.32	0.54	0.038
Wavelet-HLL GLRLM gray level variance	0.36 ± 0.37	0.62	0.014
Wavelet-HLL GLCM cluster prominence	0.26 ± 0.36	0.6	0.018
Wavelet-HLL GLCM inverse variance	0.57 ± 0.3	-0.58	0.022
Wavelet-HLL GLCM maximum probability	0.47 ± 0.35	-0.53	0.043
Wavelet-HLL GLDM dependence variance	0.41 ± 0.27	-0.6	0.018
Wavelet-HLL GLSZM size zone non uniformity	0.29 ± 0.33	0.57	0.028
Wavelet-HHH GLRLM gray level non uniformity normalized	0.74 ± 0.3	-0.54	0.039
Wavelet-HHH GLCM difference average	0.64 ± 0.31	0.56	0.03
Wavelet-HHH GLCM contrast	0.53 ± 0.28	0.64	0.009
Wavelet-HHH GLSZM small area emphasis	0.55 ± 0.33	0.69	0.005
Wavelet-HHH GLSZM small area low gray level emphasis	0.55 ± 0.33	0.59	0.022
Wavelet-HHL first order entropy	0.38 ± 0.3	0.57	0.025
Wavelet-HHL first order mean	0.64 ± 0.28	0.59	0.02
Wavelet-HHL first order mean absolute deviation	0.36 ± 0.29	0.55	0.032
Wavelet-LLH NGTDM complexity	0.16 ± 0.26	0.53	0.044
Wavelet-LLL GLDM small dependence high gray level emphasis	0.36 ± 0.3	0.56	0.031
Log-sigma-1-0-mm-3D first order root mean squared	0.43 ± 0.26	-0.51	0.049
Log-sigma-5-0-mm-3D GLRLM short run low gray level emphasis	0.22 ± 0.25	-0.52	0.047
Log-sigma-5-0-mm-3D first order 10 percentile	0.48 ± 0.39	-0.59	0.02

GLCM: Gray level co-occurrence matrix; GLDM: Gray level dependence matrix; GLRLM: Gray level run length matrix; GLSZM: Gray level size zone matrix; H: High-pass filter; L: Low-pass filter; NGTDM: Neighboring gray tone difference matrix; SD: Standard deviation.

BMI: Overall, radiogenomic analysis revealed that four of the eight mRNA regulators were significantly correlated with 10 of the 29 selected radiomic features, of which five belonging to wavelet group and three belonging to LoG sigma group as reported in **Figure 5**. In particular, METTL3 was positively correlated with HLH median, LHL GLDM high gray level emphasis, HLL GLRLM gray level variance and LLL GLDM small dependence high gray level emphasis ($\rho = 0.71$, $\rho = 0.54$, $\rho = 0.53$, $\rho = 0.6$, $P < 0.05$, respectively) and negatively correlated with HLL GLCM inverse variance and LoG sigma 10th percentile calculated with sigma = 5.0 ($\rho = -0.6$, $\rho = -0.66$, $P < 0.05$, respectively); YTHDF1 was positively correlated with wavelet feature HLL GLCM maximum probability ($\rho = 0.6$, $P < 0.05$), whereas YTHDC1 was positively correlated with the wavelet HHH GLCM difference average ($\rho = 0.67$, $P < 0.05$) and inversely

Table 4 Results of multivariate analysis for the stage I-II/stage III-IV classification task

Model order	Features involved	AUC ± SE	Sens ± SE	Spec ± SE	ACC ± SE
1	Wavelet-HHH GLCM joint entropy	0.896 ± 0.005	0.513 ± 0.021	0.865 ± 0.007	0.77 ± 0.006
2	Wavelet-LLH NGTDM complexity; Wavelet-HHH GLCM joint entropy	0.869 ± 0.008	0.643 ± 0.021	0.834 ± 0.008	0.79 ± 0.006
3	Wavelet-LLH NGTDM complexity; Wavelet-HHH GLCM joint entropy; Wavelet-HLH first order entropy	0.826 ± 0.009	0.523 ± 0.023	0.815 ± 0.009	0.744 ± 0.006
4	Wavelet-HLL GLCM cluster prominence; Wavelet-HHH GLCM joint entropy; Wavelet-LLH NGTDM complexity; Wavelet-HLH first order entropy	0.799 ± 0.009	0.668 ± 0.022	0.766 ± 0.009	0.752 ± 0.007
5	Wavelet-LLH GLDM high gray level emphasis; Wavelet-HHH GLCM joint entropy; Wavelet HLL GLCM cluster prominence; Wavelet HLH entropy; Wavelet LLH NGTDM complexity	0.724 ± 0.011	0.516 ± 0.025	0.762 ± 0.01	0.708 ± 0.008

For each model (from order 1 to 5), area under the receiver operating characteristic curve, sensitivity, specificity and accuracy were reported with the standard error on a 95%CI over all bootstrap sample. AUC: Area under the receiver operating characteristic curve; GLCM: Gray level co-occurrence matrix; GLDM: Gray level dependence matrix; GLRLM: Gray level run length matrix; GLSZM: Gray level size zone matrix; H: High-pass filter; L: Low-pass filter; NGTDM: Neighboring gray tone difference matrix; SE: Standard error.

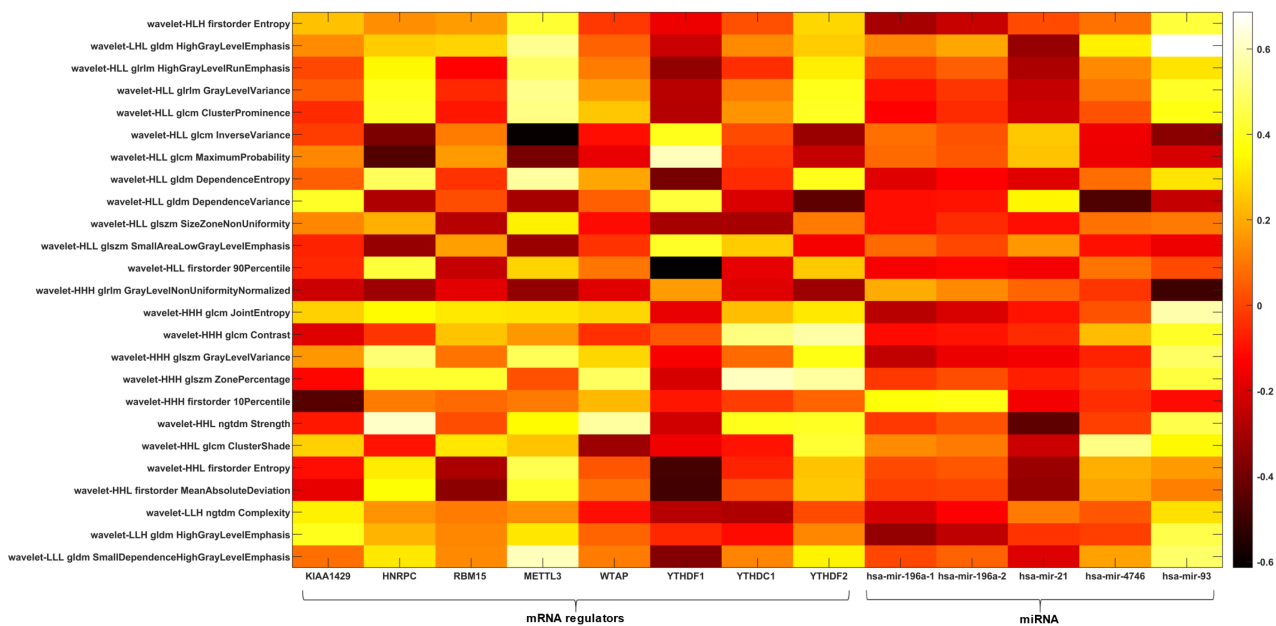


Figure 3 Radiogenomic analysis using stage as clinical outcome. Heatmap depicting the correlation matrix between transcriptomic features and radiomic features significantly associated with stage. GLCM: Gray level co-occurrence matrix; GLDM: Gray level dependence matrix; GLRLM: Gray level run length matrix; GLSZM: Gray level size zone matrix; H: High-pass filter; L: Low-pass filter; NGTDM: Neighboring gray tone difference matrix.

correlated with and LoG sigma root mean squared calculated with sigma = 1.0 ($\rho = -0.67, P < 0.05$); similarly, YTHDF2 was positively correlated with the wavelet HHH GLCM contrast ($\rho = 0.57, P < 0.05$) and inversely with the LoG sigma 10th percentile calculated with sigma = 5.0 ($\rho = -0.56, P < 0.05$). Moreover, correlation analysis with the five up-regulated miRNA revealed a significant correlation only between miRNA-93 and two radiomic features as reported in Figure 5 and in particular with the wavelet feature LHL GLRLM high gray level run emphasis ($\rho = 0.69, P < 0.05$) and the LoG sigma 10th percentile calculated with sigma = 5.0 ($\rho = -0.54, P < 0.05$).

DISCUSSION

Several studies reported that some miRNAs, such as miR-21, miR-183, miR-574-5p and miR-601, can regulate the pathways in esophageal carcinogenesis by their altered

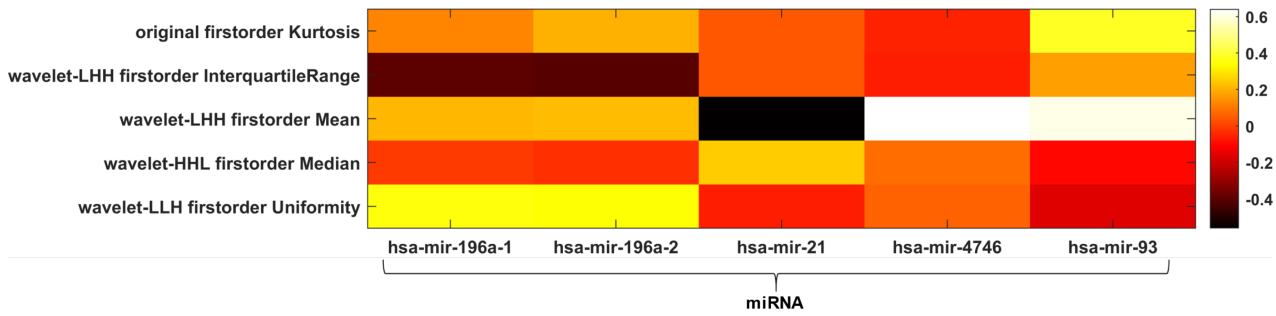


Figure 4 Radiogenomic analysis using alcohol history as clinical outcome. Heatmap depicting the correlation matrix between transcriptomic features and radiomic features significantly associated with alcohol history. H: High-pass filter; L: Low-pass filter; miRNA: MicroRNA.

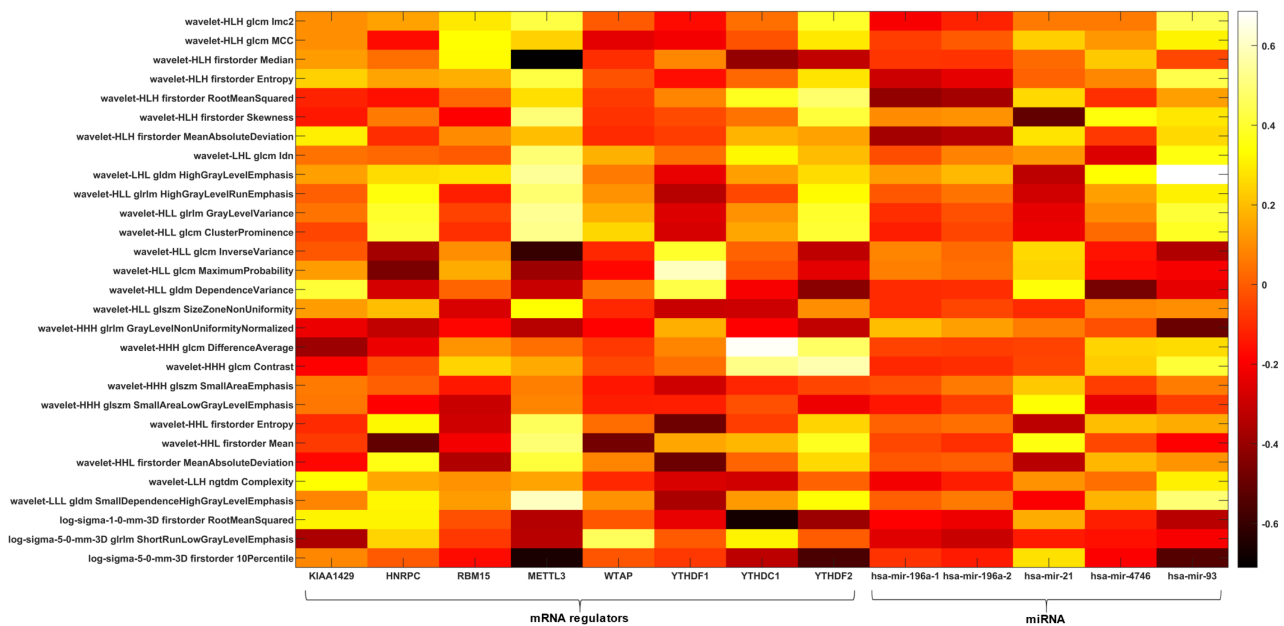


Figure 5 Radiogenomic analysis using body mass index as clinical outcome. Heatmap depicting the correlation matrix between transcriptomic features and radiomic features significantly associated with body mass index. GLCM: Gray level co-occurrence matrix; GLDM: Gray level dependence matrix; GLRLM: Gray level run length matrix; GLSZM: Gray level size zone matrix; H: High-pass filter; L: Low-pass filter; miRNA: MicroRNA; mRNA: Messenger RNA; NGTDM: Neighboring gray tone difference matrix.

expression associated with the increasing of risks factors, including dietary, smoking and drinking habits[44]. Moreover, a recent study, through an integrated approach, evaluated how dysregulated miRNAs by regulating RNA targets changed the relative miRNA-mRNA expression to survival and clinical characteristics[45]. In addition, miRNAs, more generally noncoding RNAs, have the ability to regulate m6A modifications, thereby affecting gene expression in cancer progression. Previous studies highlighted a strong relation between RNA methylation and breast cancer. In particular, Zhang *et al*[46] reported significant difference in expression levels and prognostic value of five mRNA regulators (YTHDF3, ZC3H13, LRPPRC, METTL16, RBM15B) in breast cancer. Furthermore, in a recent study, Zhao *et al*[47] showed that m6A regulator genomic aberration is associated with prognosis of ESCA patients.

It is recognized that the use of CT radiomics is rapidly increasing in the field of ESCA management, playing an important role in preoperative nodal staging, diagnosis and prognosis and for predicting treatment response to chemoradiotherapy [3,48-52]. Wu *et al*[15] showed that CT radiomic features were able to discriminate between stage I-II and III-IV ESCA. In a study by Yang *et al*[45], predictive models based on CT radiomic features were able to predict complete pathologic response after neoadjuvant chemoradiotherapy of ESCA patients. CT texture features were also found to be independent predictors of survival[48], while CT wavelet features were associated with the 3-year overall survival after chemoradiotherapy in a study involving 165 patients performed by Larue *et al*[51].

In our pilot study, we examined the relationship between the expression levels of eight m6A RNA methylation regulators (KIAA1429, HNRNPC, RBM15, METTL3, WTAP, YTHDF1, YTHDC1, YTHDF2), as well as five up-regulated miRNAs (miRNA-93, miRNA-21, miRNA-4746, miRNA-196a-1 and miRNA-196a-2) and radiomic features extracted from CT images that were significantly associated to clinical outcomes (stage, alcohol history, BMI) in patients with ESCA belonging to the public integrated datasets TCGA/TCIA. We decided to evaluate by combining radiomic and transcriptomic data the above-mentioned m6A RNA methylation regulators and up-regulated miRNA since previous studies on gene expression in ESCA found interesting results on specific mRNAs associated with tumor stage through epigenetic regulation and miRNAs signature as a prognostic biomarker[22,25].

Interestingly, both considering binary clinical outcomes (namely stage and alcohol history) and BMI, CT radiomic features that survived after radiomic feature selection were mostly belonging to the wavelet group, while only histogram Kurtosis and three LoG sigma features (one textural and two histogram features) survived after feature selection for alcohol history and BMI analysis, respectively. Wavelet features were also able to differentiate between stage I-II and III-IV ESCA, with an AUC superior to 80%. Similar performances were achieved when using the same features for predicting T and N, and this could be because T and N assignments contribute to determine the overall ESCA stage[43]. These results are in line with those found by Liu *et al*[53], even if they did not include textural features from wavelet CT images.

These results were in line with previous radiomics studies, in which CT imaging features describing tumor heterogeneity also were shown to have prognostic value in esophageal cancer[51,54]. Wavelet radiomic features from pretreatment CT were found to be useful to predict overall survival of ESCA patients after chemoradiotherapy in a study by Larue *et al*[51]. Moreover, in the work by Qiu *et al*[54], wavelet features resulted predominant in the radiomic-based predictive model developed to estimate recurrence-free survival in ESCA patients achieving a pathologic complete response.

Radiogenomic analysis performed for stage assessment revealed significant correlations between 10 wavelet textural features and six of the eight m6A RNA methylation regulators (HRNPC, WTAP, METTL3, YTHDF1, YTHDF2, YTHDC1). Moreover, correlation analysis with the five up-regulated miRNA revealed a significant positive correlation between miRNA-93 and two radiomic wavelet features, namely LHL GLDM high gray level emphasis and HHH GLCM joint entropy. It is worth to note that the wavelet feature HHH GLCM joint entropy was positively correlated with miRNA-93 and contributed to building the best predictive models for the overall stage assessment and for the assessment of the T and N categories. From the literature, miR-93 is reported to be associated in various tumors and it is recently found to regulate mechanisms of drug resistance in triple negative breast cancer[55]. Moreover, Ansari *et al*[56] evaluated miR-93 as potential deregulated biomarker for early detection of ESCA. Based on these considerations, combining genomic features with radiomic ones might be of further added value for ESCA staging, thereby influencing the personalized medicine workflow in the field of ESCA. Concerning radiogenomic analysis performed using alcohol history as clinical outcome, there were no significant associations between selected CT features and the eight m6A RNA methylation regulators, while the correlation analysis with the five up-regulated miRNA revealed a significant correlation between the wavelet feature LHH first order mean and three up-regulated miRNA, namely miRNA-21, miRNA-4746 and miRNA-93. Finally, the radiogenomic analysis on BMI revealed a significant correlation between wavelet and LoG sigma features and METTL3, YTHDF1, YTHDC1 and YTHDF2. Wavelet and LoG sigma features were also associated with miRNA-93 in radiogenomic analysis involving the five up-regulated miRNAs.

In addition, a recent study has experimentally verified that overexpression of METTL3 in tumor tissues of ESCA patients compared with normal condition from adjacent tissues is associated with metabolic status, highlighting a significant correlation with tumor size and histological differentiation; this result suggests that METTL3 may become a possible pathological index for diagnosis and a potential therapeutic target[57].

However, to our knowledge, this is the first ESCA radiogenomic study investigating the association with clinical staging and potential risk factors. Although previous radiogenomic studies were performed on ESCA[21,49,58], the strength of our study was that this is the first radiogenomic study investigating the association with stage, alcohol history, and BMI. Moreover, is not to be neglected that it is a radiogenomic study on an unexplored cancer type such as ESCA.

However, several limitations are worth noting. First, due to the extremely small sample size and the retrospective nature of the study, our results remain to be validated with a larger and prospective patient sample in the future. Second, the small sample size may have affected also prediction model performances. Therefore, a larger and more balanced study group is needed to conduct better a radiomic analysis and build more robust prediction models. In particular, although the IABR strategy we used for model building is a common reliable approach in case of small and imbalanced datasets, a larger sample size would allow using part of the dataset for the training and part for testing and validating the performance of the classifier with external datasets. In addition, it should be considered that the availability of the eight m6A RNA methylation regulators and the five up-regulated miRNAs only for a small population has prevented us from investigating other clinical outcomes, which were missing for the investigated patients. It would have been interesting to perform similar analyses considering smoking variables as clinical outcomes. In fact, in addition to alcohol, tobacco is an established risk factor for ESCA and has been proven to act synergically with alcohol to increase the risk of ESCA[59,60]. However, we could not perform analyses involving outcomes associated with smoking due to the incompleteness of these data for the included patients' cohort.

CONCLUSION

In conclusion, our preliminary study revealed interesting relationships between the expression levels of eight m6A RNA methylation regulators, as well as the five up-regulated miRNAs, and CT radiomic features that were significantly associated with clinical outcomes. Our results strengthen the role of miRNA overexpression and the possible characterization of biomarkers from liquid biopsy for ESCA assessment and staging, introducing new insights for omics integration toward a personalized medicine approach. Further prospective and retrospective studies involving larger groups of patients are essential to validate obtained results and perform in-depth analyses.

ARTICLE HIGHLIGHTS

Research background

Esophageal cancer (ESCA) is the sixth most common malignancy in the world, and its incidence is rapidly increasing. Radiogenomics provides clinically useful prognostic predictions by linking molecular characteristics such as gene mutations and gene expression patterns of malignant tumors with medical images and could provide more opportunities in the management of patients with ESCA.

Research motivation

Recently, several microRNAs (miRNAs) and messenger (RNA) targets were evaluated as potential biomarkers and regulators of epigenetic mechanisms involved in ESCA. In addition, the use of computed tomography (CT) radiomics is rapidly increasing in the field of ESCA and plays an important role in different ESCA management steps. Moreover, there are no previous radiogenomic studies on ESCA investigating the association with clinical staging and potential risk factors. This has motivated us to investigate on the relationship between the expression levels of eight N6-methyladenosine (m6A) RNA methylation regulators, as well as the five up-regulated miRNAs, and radiomic features extracted from CT images that were significantly associated to clinical outcomes.

Research objectives

To explore the combination of CT radiomic features and molecular targets associated with clinical outcomes for characterization of ESCA patients.

Research methods

Fifteen patients with diagnosed ESCA were included in this study, and their CT imaging and transcriptomic data were extracted from The Cancer Imaging Archive and gene expression data from The Cancer Genome Atlas, respectively. Cancer stage, history of significant alcohol consumption and body mass index (BMI) were

considered as clinical outcomes. Radiomic analysis was performed on CT images acquired after injection of contrast medium. In total, 1302 radiomics features were extracted from three-dimensional regions of interest by using PyRadiomics. Radiogenomic analysis involved Spearman's correlation (ρ) analysis between radiomic features associated with clinical outcomes and transcriptomic signatures consisting in eight m6A RNA methylation regulators and five up-regulated miRNA.

Research results

Radiogenomic analysis with stage as clinical outcome revealed that six of the eight mRNA regulators and two of the five up-regulated miRNA were significantly correlated with 10 and three of the 25 selected radiomic features, respectively. Assuming alcohol history as clinical outcome, no correlation was found between the five selected radiomic features and mRNA regulators, while a significant correlation was found between one radiomic feature and three up-regulated miRNA. Radiogenomic analysis with BMI as clinical outcome revealed that four mRNA regulators and one up-regulated miRNA were significantly correlated with 10 and two radiomic features, respectively.

Research conclusions

Our study revealed interesting relationships between the expression of eight m6a RNA regulators, as well as five up-regulated miRNAs, and CT radiomic features associated with clinical outcomes of ESCA patients.

Research perspectives

This preliminary study revealed interesting associations between m6a RNA regulators, as well as miRNAs, and CT radiomic features associated with clinical outcomes of ESCA patients. Further investigations on different ESCA omics data are required. Moreover, multimodal data combined with artificial intelligence techniques characteristics are desirable.

ACKNOWLEDGEMENTS

All results shown here are in whole or part based upon data generated by the TCGA Research Network: <https://www.cancer.gov/tcga>.

REFERENCES

- 1 **Bray F**, Ferlay J, Soerjomataram I, Siegel RL, Torre LA, Jemal A. Global cancer statistics 2018: GLOBOCAN estimates of incidence and mortality worldwide for 36 cancers in 185 countries. *CA Cancer J Clin* 2018; **68**: 394-424 [PMID: 30207593 DOI: 10.3322/caac.21492]
- 2 **Ahmad NR**, Goosenberg EB, Frucht H, Coia LR. Palliative Treatment of Esophageal Cancer. *Semin Radiat Oncol* 1994; **4**: 202-214 [PMID: 10717108 DOI: 10.1053/SRAO00400192]
- 3 **Yang Z**, He B, Zhuang X, Gao X, Wang D, Li M, Lin Z, Luo R. CT-based radiomic signatures for prediction of pathologic complete response in esophageal squamous cell carcinoma after neoadjuvant chemoradiotherapy. *J Radiat Res* 2019; **60**: 538-545 [PMID: 31111948 DOI: 10.1093/jrr/rrz027]
- 4 **Napier KJ**, Scheerer M, Misra S. Esophageal cancer: A Review of epidemiology, pathogenesis, staging workup and treatment modalities. *World J Gastrointest Oncol* 2014; **6**: 112-120 [PMID: 24834141 DOI: 10.4251/wjgo.v6.i5.112]
- 5 **Milsom JW**, Senagore A, Walshaw RK, Mostosky UV, Wang P, Johnson W, Chaudry IH. Preoperative radiation therapy produces an early and persistent reduction in colorectal anastomotic blood flow. *J Surg Res* 1992; **53**: 464-469 [PMID: 1434596 DOI: 10.1016/0022-4804(92)90091-d]
- 6 **Tirumani H**, Rosenthal MH, Tirumani SH, Shinagare AB, Krajewski KM, Ramaiya NH. Esophageal Carcinoma: Current Concepts in the Role of Imaging in Staging and Management. *Can Assoc Radiol J* 2015; **66**: 130-139 [PMID: 25770628 DOI: 10.1016/j.carj.2014.08.006]
- 7 **Elsherif SB**, Andreou S, Virarkar M, Soule E, Gopireddy DR, Bhosale PR, Lall C. Role of precision imaging in esophageal cancer. *J Thorac Dis* 2020; **12**: 5159-5176 [PMID: 33145093 DOI: 10.21037/jtd.2019.08.15]
- 8 **Umeoka S**, Koyama T, Togashi K, Saga T, Watanabe G, Shimada Y, Imamura M. Esophageal cancer: evaluation with triple-phase dynamic CT--initial experience. *Radiology* 2006; **239**: 777-783 [PMID: 16621930 DOI: 10.1148/radiol.2393050222]
- 9 **Sultan R**, Haider Z, Chawla TU. Diagnostic accuracy of CT scan in staging resectable esophageal cancer. *J Pak Med Assoc* 2016; **66**: 90-92 [PMID: 26712189]
- 10 **Lambin P**, Rios-Velazquez E, Leijenaar R, Carvalho S, van Stiphout RG, Granton P, Zegers CM,

- Gillies R, Boellard R, Dekker A, Aerts HJ. Radiomics: extracting more information from medical images using advanced feature analysis. *Eur J Cancer* 2012; **48**: 441-446 [PMID: 2257792 DOI: 10.1016/j.ejca.2011.11.036]
- 11 Gillies RJ, Kinahan PE, Hricak H. Radiomics: Images Are More than Pictures, They Are Data. *Radiology* 2016; **278**: 563-577 [PMID: 26579733 DOI: 10.1148/radiol.2015151169]
 - 12 van Rossum PSN, Xu C, Fried DV, Goense L, Court LE, Lin SH. The emerging field of radiomics in esophageal cancer: current evidence and future potential. *Transl Cancer Res* 2016; **5**: 410-423 [PMID: 30687593 DOI: 10.21037/tcr.2016.06.19]
 - 13 Rizzo S, Botta F, Raimondi S, Origgi D, Fanciullo C, Morganti AG, Bellomi M. Radiomics: the facts and the challenges of image analysis. *Eur Radiol Exp* 2018; **2**: 36 [PMID: 30426318 DOI: 10.1186/s41747-018-0068-z]
 - 14 Hou T-C, Huang W-C, Tai H-C, Chen Y-J. Integrated radiomic model for predicting the prognosis of esophageal squamous cell carcinoma patients undergoing neoadjuvant chemoradiation. *Ther Radiol Oncol* 2019; **3**: 28 [DOI: 10.21037/tro.2019.07.03]
 - 15 Wu L, Wang C, Tan X, Cheng Z, Zhao K, Yan L, Liang Y, Liu Z, Liang C. Radiomics approach for preoperative identification of stages I-II and III-IV of esophageal cancer. *Chin J Cancer Res* 2018; **30**: 396-405 [PMID: 30210219 DOI: 10.21147/j.issn.1000-9604.2018.04.02]
 - 16 Jin X, Zheng X, Chen D, Jin J, Zhu G, Deng X, Han C, Gong C, Zhou Y, Liu C, Xie C. Prediction of response after chemoradiation for esophageal cancer using a combination of dosimetry and CT radiomics. *Eur Radiol* 2019; **29**: 6080-6088 [PMID: 31028447 DOI: 10.1007/s00330-019-06193-w]
 - 17 Hyman DM, Taylor BS, Baselga J. Implementing Genome-Driven Oncology. *Cell* 2017; **168**: 584-599 [PMID: 28187282 DOI: 10.1016/j.cell.2016.12.015]
 - 18 Berger MF, Mardis ER. The emerging clinical relevance of genomics in cancer medicine. *Nat Rev Clin Oncol* 2018; **15**: 353-365 [PMID: 29599476 DOI: 10.1038/s41571-018-0002-6]
 - 19 Guo W, Jiang YG. Current gene expression studies in esophageal carcinoma. *Curr Genomics* 2009; **10**: 534-539 [PMID: 20514215 DOI: 10.2174/138920209789503888]
 - 20 Visser E, Franken IA, Brosens LA, Ruurda JP, van Hillegersberg R. Prognostic gene expression profiling in esophageal cancer: a systematic review. *Oncotarget* 2017; **8**: 5566-5577 [PMID: 27852047 DOI: 10.18632/oncotarget.13328]
 - 21 Hoshino I, Yokota H, Ishige F, Iwatate Y, Takeshita N, Nagase H, Uno T, Matsubara H. Radiogenomics predicts the expression of microRNA-1246 in the serum of esophageal cancer patients. *Sci Rep* 2020; **10**: 2532 [PMID: 32054931 DOI: 10.1038/s41598-020-59500-7]
 - 22 Zeng JH, Xiong DD, Pang YY, Zhang Y, Tang RX, Luo DZ, Chen G. Identification of molecular targets for esophageal carcinoma diagnosis using miRNA-seq and RNA-seq data from The Cancer Genome Atlas: a study of 187 cases. *Oncotarget* 2017; **8**: 35681-35699 [PMID: 28415685 DOI: 10.18632/oncotarget.16051]
 - 23 Ma S, Chen C, Ji X, Liu J, Zhou Q, Wang G, Yuan W, Kan Q, Sun Z. The interplay between m6A RNA methylation and noncoding RNA in cancer. *J Hematol Oncol* 2019; **12**: 121 [PMID: 31757221 DOI: 10.1186/s13045-019-0805-7]
 - 24 Lan Q, Liu PY, Haase J, Bell JL, Hüttelmaier S, Liu T. The Critical Role of RNA m⁶A Methylation in Cancer. *Cancer Res* 2019; **79**: 1285-1292 [PMID: 30894375 DOI: 10.1158/0008-5472.CAN-18-2965]
 - 25 Xu LC, Pan JX, Pan HD. Construction and Validation of an m6A RNA Methylation Regulators-Based Prognostic Signature for Esophageal Cancer. *Cancer Manag Res* 2020; **12**: 5385-5394 [PMID: 32753956 DOI: 10.2147/CMAR.S254870]
 - 26 Sah BR, Owczarczyk K, Siddique M, Cook GJR, Goh V. Radiomics in esophageal and gastric cancer. *Abdom Radiol (NY)* 2019; **44**: 2048-2058 [PMID: 30116873 DOI: 10.1007/s00261-018-1724-8]
 - 27 Klaassen R, Larue RTHM, Mearadji B, van der Woude SO, Stoker J, Lambin P, van Laarhoven HWM. Feasibility of CT radiomics to predict treatment response of individual liver metastases in esophagogastric cancer patients. *PLoS One* 2018; **13**: e0207362 [PMID: 30440002 DOI: 10.1371/journal.pone.0207362]
 - 28 Wu R, Zhuang H, Mei YK, Sun JY, Dong T, Zhao LL, Fan ZN, Liu L. Systematic identification of key functional modules and genes in esophageal cancer. *Cancer Cell Int* 2021; **21**: 134 [PMID: 33632229 DOI: 10.1186/s12935-021-01826-x]
 - 29 Peng Q, Chen H, Huo JR. Alcohol consumption and corresponding factors: A novel perspective on the risk factors of esophageal cancer. *Oncol Lett* 2016; **11**: 3231-3239 [PMID: 27123096 DOI: 10.3892/ol.2016.4401]
 - 30 Long E, Beales IL. The role of obesity in oesophageal cancer development. *Therap Adv Gastroenterol* 2014; **7**: 247-268 [PMID: 25364384 DOI: 10.1177/1756283X14538689]
 - 31 Turati F, Tramacere I, La Vecchia C, Negri E. A meta-analysis of body mass index and esophageal and gastric cardia adenocarcinoma. *Ann Oncol* 2013; **24**: 609-617 [PMID: 22898040 DOI: 10.1093/annonc/mds244]
 - 32 Lucchesi FR, Aredes ND. Radiology Data from The Cancer Genome Atlas Esophageal Carcinoma [TCGA-ESCA] collection. *The Cancer Imaging Archive* 2016 [DOI: 10.7937/K9/TCIA.2016.VPTNRGFY]
 - 33 Clark K, Vendt B, Smith K, Freymann J, Kirby J, Koppel P, Moore S, Phillips S, Maffitt D, Pringle M, Tarbox L, Prior F. The Cancer Imaging Archive (TCIA): maintaining and operating a public information repository. *J Digit Imaging* 2013; **26**: 1045-1057 [PMID: 23884657 DOI: 10.1007/s10278-013-9622-7]

- 34 **Zwanenburg A**, Vallières M, Abdalah MA, Aerts HJWL, Andrearczyk V, Apte A, Ashrafinia S, Bakas S, Beukinga RJ, Boellaard R, Bogowicz M, Boldrini L, Buvat I, Cook GJR, Davatzikos C, Depeursinge A, Desseroit MC, Dinapoli N, Dinh CV, Echegaray S, El Naqa I, Fedorov AY, Gatta R, Gillies RJ, Goh V, Götz M, Guckenberger M, Ha SM, Hatt M, Isensee F, Lambin P, Leger S, Leijenaar RTH, Lenkiewicz J, Lippert F, Losnegård A, Maier-Hein KH, Morin O, Müller H, Napel S, Nioche C, Orlhac F, Pati S, Pfähler EAG, Rahmim A, Rao AUK, Scherer J, Siddique MM, Sijtsema NM, Socarras Fernandez J, Spezi E, Steenbakkers RJHM, Tanadini-Lang S, Thorwarth D, Troost EGC, Upadhyaya T, Valentini V, van Dijk LV, van Griethuysen J, van Velden FHP, Whybra P, Richter C, Löck S. The Image Biomarker Standardization Initiative: Standardized Quantitative Radiomics for High-Throughput Image-based Phenotyping. *Radiology* 2020; **295**: 328-338 [PMID: [32154773](#) DOI: [10.1148/radiol.2020191145](#)]
- 35 **Vergara JR**, Estévez PA. A review of feature selection methods based on mutual information. *Neural Comput Applic* 2014; **24**: 175-186 [DOI: [10.1007/s00521-013-1368-0](#)]
- 36 **Zaffalon M**, Hutter M. Robust Feature Selection by Mutual Information Distributions. 2014 Preprint. Available from: arXiv: 1408.1487v1
- 37 **Roffo G**. Feature Selection Library (MATLAB Toolbox). 2018 Preprint. Available from: arXiv: 1607.01327v5
- 38 **Vallières M**, Freeman CR, Skamene SR, El Naqa I. A radiomics model from joint FDG-PET and MRI texture features for the prediction of lung metastases in soft-tissue sarcomas of the extremities. *Phys Med Biol* 2015; **60**: 5471-5496 [PMID: [26119045](#) DOI: [10.1088/0031-9155/60/14/5471](#)]
- 39 **Efron B**. Bootstrap Methods: Another Look at the Jackknife. *Ann Statist* 1979; **7**: 1-26 [DOI: [10.1214/aos/1176344552](#)]
- 40 **Efron B**, Tibshirani R. Improvements on Cross-Validation: The .632+ Bootstrap Method. *J Am Stat Assoc* 1997; **92**: 548 [DOI: [10.2307/2965703](#)]
- 41 **Brancato V**, Aiello M, Basso L, Monti S, Palumbo L, Di Costanzo G, Salvatore M, Ragozzino A, Cavaliere C. Evaluation of a multiparametric MRI radiomic-based approach for stratification of equivocal PI-RADS 3 and upgraded PI-RADS 4 prostatic lesions. *Sci Rep* 2021; **11**: 643 [PMID: [33436929](#) DOI: [10.1038/s41598-020-80749-5](#)]
- 42 **Sahiner B**, Chan HP, Hadjiiski L. Classifier performance prediction for computer-aided diagnosis using a limited dataset. *Med Phys* 2008; **35**: 1559-1570 [PMID: [18491550](#) DOI: [10.1118/1.2868757](#)]
- 43 **Berry MF**. Esophageal cancer: staging system and guidelines for staging and treatment. *J Thorac Dis* 2014; **6** Suppl 3: S289-S297 [PMID: [24876933](#) DOI: [10.3978/j.issn.2072-1439.2014.03.11](#)]
- 44 **Stánitz É**, Juhász K, Gombos K, Gócze K, Tóth C, Kiss I. Alteration of miRNA expression correlates with lifestyle, social and environmental determinants in esophageal carcinoma. *Anticancer Res* 2015; **35**: 1091-1097 [PMID: [25667498](#)]
- 45 **Yang H**, Su H, Hu N, Wang C, Wang L, Giffen C, Goldstein AM, Lee MP, Taylor PR. Integrated analysis of genome-wide miRNAs and targeted gene expression in esophageal squamous cell carcinoma (ESCC) and relation to prognosis. *BMC Cancer* 2020; **20**: 388 [PMID: [32375686](#) DOI: [10.1186/s12885-020-06901-6](#)]
- 46 **Zhang B**, Gu Y, Jiang G. Expression and Prognostic Characteristics of m⁶ A RNA Methylation Regulators in Breast Cancer. *Front Genet* 2020; **11**: 604597 [PMID: [33362863](#) DOI: [10.3389/fgene.2020.604597](#)]
- 47 **Zhao H**, Xu Y, Xie Y, Zhang L, Gao M, Li S, Wang F. m6A Regulators Is Differently Expressed and Correlated With Immune Response of Esophageal Cancer. *Front Cell Dev Biol* 2021; **9**: 650023 [PMID: [33748145](#) DOI: [10.3389/fcell.2021.650023](#)]
- 48 **Ganeshan B**, Skogen K, Pressney I, Coutroubis D, Miles K. Tumour heterogeneity in oesophageal cancer assessed by CT texture analysis: preliminary evidence of an association with tumour metabolism, stage, and survival. *Clin Radiol* 2012; **67**: 157-164 [PMID: [21943720](#) DOI: [10.1016/j.crad.2011.08.012](#)]
- 49 **Hu Y**, Xie C, Yang H, Ho JWK, Wen J, Han L, Chiu KWH, Fu J, Vardhanabhuti V. Assessment of Intratumoral and Peritumoral Computed Tomography Radiomics for Predicting Pathological Complete Response to Neoadjuvant Chemoradiation in Patients With Esophageal Squamous Cell Carcinoma. *JAMA Netw Open* 2020; **3**: e2015927 [PMID: [32910196](#) DOI: [10.1001/jamanetworkopen.2020.15927](#)]
- 50 **Piazzese C**, Foley K, Whybra P, Hurt C, Crosby T, Spezi E. Discovery of stable and prognostic CT-based radiomic features independent of contrast administration and dimensionality in oesophageal cancer. *PLoS One* 2019; **14**: e0225550 [PMID: [31756181](#) DOI: [10.1371/journal.pone.0225550](#)]
- 51 **Larue RTHM**, Klaassen R, Jochems A, Leijenaar RTH, Hulshof MCCM, van Berge Henegouwen MI, Schreurs WMJ, Sosef MN, van Elmpt W, van Laarhoven HWM, Lambin P. Pre-treatment CT radiomics to predict 3-year overall survival following chemoradiotherapy of esophageal cancer. *Acta Oncol* 2018; **57**: 1475-1481 [PMID: [30067421](#) DOI: [10.1080/0284186X.2018.1486039](#)]
- 52 **Hou Z**, Yang Y, Li S, Yan J, Ren W, Liu J, Wang K, Liu B, Wan S. Radiomic analysis using contrast-enhanced CT: predict treatment response to pulsed low dose rate radiotherapy in gastric carcinoma with abdominal cavity metastasis. *Quant Imaging Med Surg* 2018; **8**: 410-420 [PMID: [29928606](#) DOI: [10.21037/qims.2018.05.01](#)]
- 53 **Liu S**, Zheng H, Pan X, Chen L, Shi M, Guan Y, Ge Y, He J, Zhou Z. Texture analysis of CT imaging for assessment of esophageal squamous cancer aggressiveness. *J Thorac Dis* 2017; **9**: 4724-4732 [DOI: [10.21037/jtd.2017.06.46](#)]
- 54 **Qiu Q**, Duan J, Deng H, Han Z, Gu J, Yue NJ, Yin Y. Development and Validation of a Radiomics

- Nomogram Model for Predicting Postoperative Recurrence in Patients With Esophageal Squamous Cell Cancer Who Achieved pCR After Neoadjuvant Chemoradiotherapy Followed by Surgery. *Front Oncol* 2020; **10**: 1398 [PMID: 32850451 DOI: 10.3389/fonc.2020.01398]
- 55 **Qattan A**, Al-Tweigeri T, Alkhalil W, Suleman K, Tulbah A, Amer S. Clinical Identification of Dysregulated Circulating microRNAs and Their Implication in Drug Response in Triple Negative Breast Cancer (TNBC) by Target Gene Network and Meta-Analysis. *Genes* 2021; **12**: 549 [DOI: 10.3390/genes12040549]
- 56 **Ansari MH**, Irani S, Edalat H, Amin R, Mohammadi Roushandeh A. Deregulation of miR-93 and miR-143 in human esophageal cancer. *Tumor Biol* 2016; **37**: 3097-3103 [DOI: 10.1007/s13277-015-3987-9]
- 57 **Liu XS**, Yuan LL, Gao Y, Zhou LM, Yang JW, Pei ZJ. Overexpression of METTL3 associated with the metabolic status on ¹⁸F-FDG PET/CT in patients with Esophageal Carcinoma. *J Cancer* 2020; **11**: 4851-4860 [PMID: 32626532 DOI: 10.7150/jca.44754]
- 58 **Hu Y**, Xie C, Yang H, Ho JWK, Wen J, Han L, Lam KO, Wong IYH, Law SYK, Chiu KWH, Vardhanabhuti V, Fu J. Computed tomography-based deep-learning prediction of neoadjuvant chemoradiotherapy treatment response in esophageal squamous cell carcinoma. *Radiother Oncol* 2021; **154**: 6-13 [PMID: 32941954 DOI: 10.1016/j.radonc.2020.09.014]
- 59 **Prabhu A**, Obi KO, Rubenstein JH. The synergistic effects of alcohol and tobacco consumption on the risk of esophageal squamous cell carcinoma: a meta-analysis. *Am J Gastroenterol* 2014; **109**: 822-827 [PMID: 24751582 DOI: 10.1038/ajg.2014.71]
- 60 **Dong J**, Thrift AP. Alcohol, smoking and risk of oesophago-gastric cancer. *Best Pract Res Clin Gastroenterol* 2017; **31**: 509-517 [PMID: 29195670 DOI: 10.1016/j.bpg.2017.09.002]



Published by **Baishideng Publishing Group Inc**
7041 Koll Center Parkway, Suite 160, Pleasanton, CA 94566, USA
Telephone: +1-925-3991568
E-mail: bpgoffice@wjgnet.com
Help Desk: <https://www.f6publishing.com/helpdesk>
<https://www.wjgnet.com>

